https://doi.org/10.1070/QEL16484

QML-generation dynamics of a solid-state laser with an acousto-optic travelling wave modulator

O.E. Nanii, A.I. Odintsov, A.I. Panakov, A.P. Smirnov, A.I. Fedoseev

Abstract. **The features of the generation dynamics of a laser with an acousto-optic modulator are studied. The light field injection with a frequency shift from the previous mode to the subsequent one ensures mode locking, and in many cases contributes to the instability and self-oscillations at the laser relaxation frequency. The amplitude and frequency characteristics of the emerging regime, along with the features of the regimes realised under external modulation of the diffraction coupling coefficient, are analysed.**

Keywords: *laser, mode locking, Q-switching, acousto-optic modulator, self-oscillations, relaxation frequency.*

1. Introduction

Trains of short optical pulses with a high peak power are used in time-resolution spectroscopy, optical tomography for high-precision material processing, measurement technology and other fields. Promising sources of such radiation are solid-state, simultaneously Q-switched and mode-locked lasers or so-called QML lasers. Simultaneously mode-locked and Q-switched lasers have significant advantages in the applications requiring precise synchronisation of generated pulses with other devices.

In the first QML lasers, two acousto-optic modulators (AOMs) were used in the resonator [1]. Mode-locking was provided by means of a standing acoustic wave AOM, while Q-switching was ensured by a travelling wave AOM. Kornienko et al. [2] proposed to use the return of the wave diffracted in the AOM back to the acousto-optic interaction region, which substantially increased the modulation efficiency and allowed one to implement the stationary mode-locking when the travelling wave AOM was used in the resonator [3, 4]. Thus, Kravstov et al. [3] used additional mirrors to return the diffracted radiation to the resonator, while Nadtocheev and Nanii [4] applied a V-shaped resonator of special design for the same purpose. The possibility of combining the mode-locking and Q-switching regimes using a single travelling wave AOM is demonstrated in paper [5], in which the QML regime was observed at a high transmission of the resonator plane output mirror in a Nd:YVO_4 laser.

O.E. Nanii, A.I. Odintsov, A.I. Panakov, A.I. Fedoseev Faculty of Physics, M.V. Lomonosov Moscow State University, Vorob'evy Gory, 119991 Moscow, Russia; e-mail: naniy@t8.ru, fedoseev362@mail.ru; **A.P. Smirnov** Faculty of Computational Mathematics and Cybernetics, M.V. Lomonosov Moscow State University, Vorob'evy Gory, 119991 Moscow, Russia

Received 25 July 2017
Kvantovaya Elektronika **47** (11) 1000–1004 (2017)
Translated by M.A. Monastyrskiy

A stable QML regime in a Nd:YAG laser has been implemented experimentally with a single travelling wave AOM located at the curvature centre of a highly reflecting spherical mirror [6, 7] under a double Bragg angle θ_B relative to the resonator axis (Fig. 1). A wave that has not experienced diffraction with a frequency ν_0 and also a wave that has experienced double diffraction with a frequency $\nu_0 + 2f$ (f is the modulator operating frequency) return to the resonator. Mode-locking emerges at the modulator operating frequency f equal to half the intermode interval. Waves with frequencies $\nu_0 \pm f$, which have only experienced a single diffraction, leave the resonator, thus determining additional losses associated with the AOM. A rapid decrease in additional losses occurs during the attenuation process of the sound wave. Thus, when the AOM operating frequency is switched off, the resonator Q-factor is modulated. It was later found experimentally [8] that the Q-switching regime may occur 'spontaneously' at the laser relaxation frequency at a constant amplitude of the acoustic wave. These experimental studies have shown that under certain conditions a steady-state mode-locking regime becomes unstable, and a build-up of relaxation oscillations becomes possible.

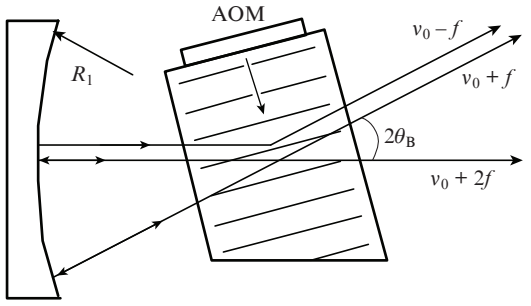

Figure 1. Scheme of the QML regime implementation in a Nd:YAG laser.

In this paper, we investigate the QML-generation dynamics in a solid-state laser with a travelling wave AOM in a scheme similar to that shown in Fig. 1. The developed numerical model makes it possible to establish the build-up limits of self-oscillations at the relaxation frequency and to study the main properties of the generation dynamics of an active QML laser.

2. Model and equations

The proposed model uses a modal approach based on fundamental works on the theory of stimulated amplitude modula-

tion [9, 10]. The amplification line is assumed uniformly broadened, and the amplification saturation is assumed homogeneous over space. Provided that the main mode frequency ($j = 0$) coincides with the amplification line centre, this makes it possible to take into account the dependence of the cross section of the optical transition σ_j only on the mode number j: $\sigma_j/\sigma_0 = (1 + j^2b^2)$, $b = \delta\nu_c/\delta\nu_g$, where $\delta\nu_c = c/(2L)$ is the intermode interval, and $\delta\nu_g$ is the amplification line width.

It is accepted that the active medium is characterised by a unified inversion relaxation time, and the medium saturation is determined by the total intensity $\bar{I}$ of modes, averaged over a time being much longer than the round-trip time of light in the resonator. In the calculations of the dynamic generation regimes, it is assumed that the radiation intensity cannot fall below the level of spontaneous emission into a mode.

It is also accepted that the field attenuation rate in the resonator is determined by the constant losses γ and the variable losses γ_d that are AOM-associated. The magnitude of the constant losses is $\gamma = -\ln(1-\theta)/T_c$, where θ is determined by the losses on the resonator's optical elements, and T_c is the round-trip time of light in the resonator. The value of γ_d is found from the balance of the wave intensities schematically shown in Fig. 1: $\gamma_d = -\ln(1-\kappa_d^2)/T_c$. Here, κ_d is the diffraction coupling coefficient equal to the fraction of the light field reflected from the acoustic wave in the AOM. The same coefficient determines the rate of diffraction injection of the field from the mode $j-1$ into the mode j: $\xi = \kappa_d^2/T_c$.

Within the framework of the assumptions made, the equations for the normalised complex amplitudes of the fields $\tilde{E}_j$ have the form (see [11]):

$$\frac{d}{d\tau}\tilde{E}_j = \left[\frac{\gamma T_1}{2}\left(\frac{\sigma_j}{\sigma_0}n - 1\right) - \gamma_d T_1\right]\tilde{E}_j + \xi T_1 \tilde{E}_{j-1}. \quad (1)$$

Here, $\tau = t/T_1$ is the normalised time (T_1 is the inversion relaxation time). In the equation for the fundamental mode, $j = 0$, $\xi = 0$ and $\sigma_j = \sigma_0$.

The intensity I as a function of time τ is calculated as the square of the complex field modulus:

$$I = \left|\sum_j E_j \exp[i(j\delta\hat{\omega}_c\tau + \varphi_j)]\right|^2, \quad (2)$$

where $\delta\hat{\omega}_c = 2\pi\delta\nu_c T_1$; and φ_j is the mode field phase with the number j.

A system of equations for normalised real quantities is used in numerical calculations:

$$\frac{d}{d\tau}E_0 = \frac{\gamma T_1}{2}E_0(n-1) - \gamma_d T_1 E_0, \quad (3)$$

$$\frac{d}{d\tau}E_j = \left[\frac{\gamma T_1}{2}\left(\frac{\sigma_j}{\sigma_0}n - 1\right) - \gamma_d T_1\right]E_j + \xi T_1 E_{j-1}\cos\Phi_j, \quad (4)$$

$$\frac{d}{d\tau}\varphi_j = T_1\xi\frac{E_{j-1}}{E_j}\sin\Phi_j. \quad (5)$$

Here, $\Phi_j = \delta\hat{\omega}\tau + \varphi_{j-1} - \varphi_j$ determines the phase shift due to the AOM detuning from the intermode frequency interval ($\varphi_0 = 0$ was assumed in in the calculations), and $\delta\hat{\omega} = 2\pi\delta\nu T_1$ is the value of detuning.

A balance equation for the normalised inversion n is added to the field equations:

$$\frac{d}{d\tau}n = \eta - n\left(1 + \sum_j |E_j|^2\frac{\sigma_j}{\sigma_0}\right), \quad (6)$$

where η is the pump parameter, which determines the inversion excess over the threshold corresponding to the level of the constant losses in the resonator.

Most calculations are performed for the numerical values of the parameters typical for a Nd:YAG laser: $T_1 = 2 \times 10^{-4}$ s, $1/\gamma = 4 \times 10^{-7}$ s, $\delta\nu_c = 200$ MHz, $\delta\nu_g = 100$ GHz.

3. Results and discussion

3.1. Dynamics of the averaged intensity with an unchanged diffractive coupling coefficient κ_d

The implementation of the QML regime is associated with the dynamics of averaged intensity

$$\bar{I}(\tau) = \sum_j |E_j|^2\frac{\sigma_j}{\sigma_0},$$

since it is this value that determines the dynamics common for all inversion modes (hereafter the results of calculations are given under the condition that the AOM operating frequency is accurately tuned to resonances). The behaviour of $\bar{I}(\tau)$ depends on the number and composition of the modes participating in lasing. A characteristic feature of the system under study is an unusual distribution of the intensities of the modes E_j^2 over the spectrum: the spectrum maximum is shifted relative to the amplification maximum, and the offset value depends nonmonotonically on the normalised coefficient κ_d. Such distributions calculated for stationary solutions of Eqns (3)–(6) are shown in Fig. 2. For each value of κ_d, the presence of a maximum is stipulated by the existence of two competing factors – field injection into subsequent modes and a decrease in amplification with increasing mode number j. With increasing κ_d, diffraction losses also increase and, therefore, the intensities of all modes fall, and the shift of the distribution maximum to the right (towards larger j) slows down and then changes to a shift to the left. This peculiarity allows us to limit the number of modes considered in the numerical experiment. The calculations do not take into account the fields of modes, the amplitude of which is less than one thou-

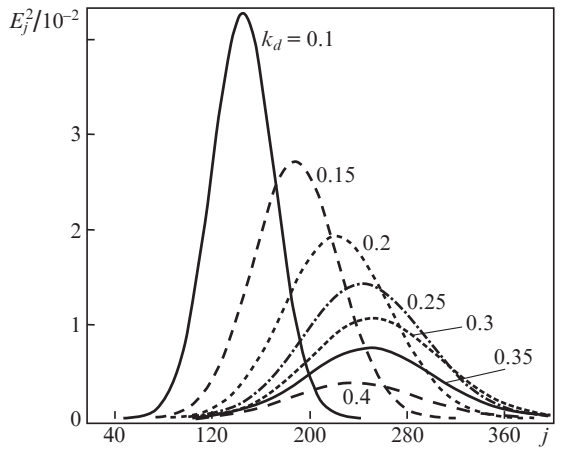

Figure 2. Stationary frequency profiles E_j^2 for different values of κ_d (pump parameter $\eta = 6$).

sandth of the maximum amplitude. In most calculations, this condition was satisfied for $j_{max} = 400$.

Our calculations performed for the sets of parameters given in work [8] show that the stationary solutions of expressions (3)–(6) are unstable, and self-oscillations $\bar{I}(\tau)$ arise at the relaxation frequency. This agrees with the experimental data of [8], with the instability zone turning out sufficiently wide with respect to the system parameters.

Figure 3 shows the instability zone $\bar{I}(\tau)$ in the coordinates η, κ_d with the other parameters unchanged. This zone expands with increasing η. It can be assumed that the instability is associated with the process of successive field injections. The equilibrium between the field of the fundamental mode E_0, operating in the amplification saturation regime, and the fields of the remaining modes operating in the regenerative amplification regime, turns out unstable. For example, a small disturbance of the stationary field E_0 contributes to the process of field injection into the subsequent modes. The effect on the inversion common for all the modes may prove to be such that an even greater opposite-sign perturbation arises. In this case, small oscillations at the laser relaxation frequency increase, thereby forming a saturated self-oscillatory regime. In this case, the stabilising factor near the lower (relative to the value of κ_d) boundary of the instability zone is a deep saturation of the medium, which occurs in the case of stationary generation. On the upper boundary, the impact of the injection process can be weakened by an increased diffraction loss. Thus, the coefficient κ_d may serve as a control parameter, the change of which makes it possible to control the dynamic generation regimes.

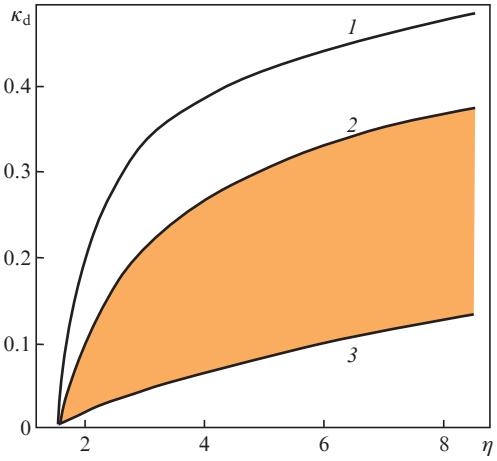

Figure 3. Boundaries of (*1*) generation and (*2*, *3*) instability zones.

Figure 4 shows the characteristics of the self-modulation regime for the pump parameter $\eta = 5.5$. At low values of κ_d, relaxation oscillations with low values of $\bar{I}_{max}$, which weakly saturate the medium, are observed. Their frequency is relatively high ($\nu_r \approx 8$) due to a significant excess of amplification above the threshold. As the value of κ_d grows and the instability develops, $\bar{I}_{max}$ rapidly increases and self-oscillations saturate the medium. In this case, the frequency of relaxation oscillations decreases sharply as a result of the medium saturation (it is known that the frequency of the relaxation oscillations saturating the medium is always lower than the frequency of small oscillations). The presence of a maximum on the intensity curve is due to the impact of increasing diffraction losses. Their further increase leads to a decrease in the value of $\bar{I}_{max}$ and the medium saturation depth, and, as a consequence, to the growth of ν_r.

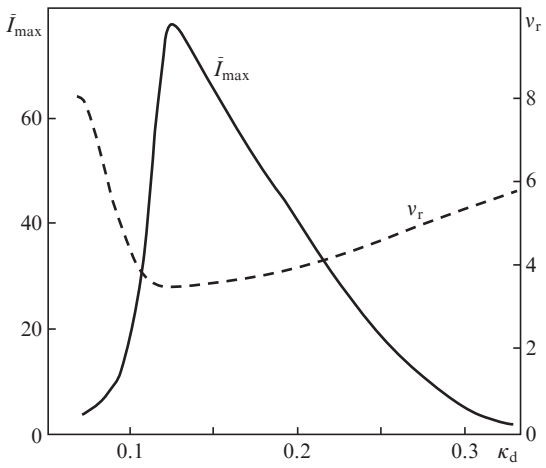

Figure 4. Self-modulation regime characteristics: pulse amplitude $\bar{I}_{max}$ and repetition rate ν_r.

The transient process, to which a small instantaneous decrease in κ_d (by a value of $\sim 10^{-3}$) leads inside the stability region, demonstrates an aperiodic 'burst' of intensity and is characterised by a rather short time ($\sim 10^{-1}$). In this case, the frequency profile changes insignificantly with time, although the maxima of the mode intensities are attained at different time moments. Figure 5 shows the transient process with a relatively smooth transition from the stability region with $\kappa_d = 0.35$ to the instability region with $\kappa_d = 0.2$ for $\eta = 5.5$. Significant inversion oscillations in this process lead to the appearance of pulses that saturate the medium. The establishment time for saturated relaxation oscillations after the completion of the changes in κ_d is also sufficiently small and amounts to $\sim 0.3\tau$.

The short times of transient processes makes it possible to effectively change the dynamic generation regime. At the same time, it follows from Fig. 4 that for a given pump parameter, high values of $\bar{I}_{max}$ are attained in a rather narrow range of κ_d values and pulse repetition rates. This narrows the possibilities of obtaining repetitively pulsed generation with a

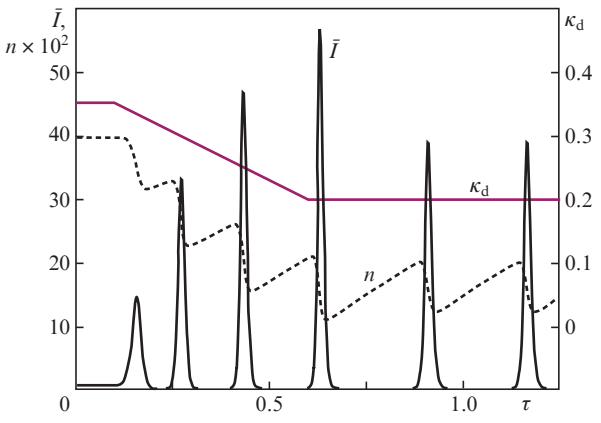

Figure 5. Transient process with a smooth change of the control parameter κ_d.

high amplitude of pulses. It is possible to increase the value of $\bar{I}_{max}$ and broaden the range of pulse repetition rates by periodic 'external' Q-switching of the resonator. To this end, the coefficient κ_d is modulated at relatively low frequencies from high values (stable generation or its absence) to minimum values at which the AOM functions are still performed.

3.2. Dynamics of averaged intensity with κ_d modulation

We consider harmonic modulation of the diffraction coupling coefficient at the frequencies which are not too large compared to the frequency ν_r: $\kappa_d(\tau) = \kappa_d[1 + A\sin(2\pi\nu_m\tau)]$, where A is the modulation amplitude and ν_m is the modulation frequency. Figure 6 shows the dependence of the pulse repetition rate ν_p on the modulation frequency ν_m. Regular pulsations of $\bar{I}$ appear in the frequency bands near $\nu_r \approx 2.2$. These bands correspond to the ranges of ν_m variation, marked with numbers 1, 2 and 3. In the intervals between these ranges, the modes with a complicated period and chaotic generation are observed. The measured correlation dimensions ρ_{cor} of the corresponding chaotic attractors turned out to be close to 1.5. For $\nu_m \gg \nu_r$, the ranges of regular pulsations are narrowed, and then the pulses of a much smaller amplitude with a repetition frequency of ν_m appear at large modulation frequencies.

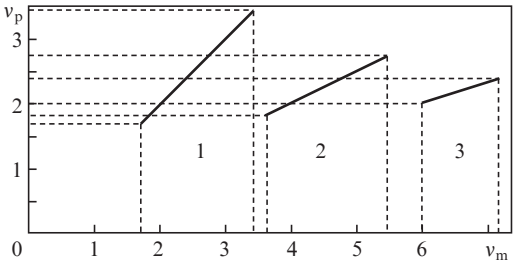

Figure 6. Dependence of the pulse repetition rate ν_p on the frequency ν_m at harmonic modulation κ_d in the range 0.4–0.2 ($\eta = 5.5$).

The relaxation frequency ν_r changes within a small range with variation of $\kappa_d(\tau)$. In the case represented in Fig. 6, we can talk about the signal interaction at frequency ν_p with a sufficiently broad relaxation resonance. In range 1, the value of ν_m varies near the resonance and, therefore, $\nu_p = \nu_m$. The generation pulse periodically emerges at a time moment close to the minimum of $\kappa_d(\tau)$, when the increasing inversion value n exceeds a threshold. Therefore, in the ranges of regular pulsations, the frequency ratio ν_m/ν_r is an integer. The transition of the frequency ν_m from one range to another (for example, from 2 to 3) leads to a decrease in the generation frequency by an integer factor and (with increasing range number) to a 'contraction' of the regular generation band to the relaxation resonance. Figure 7 shows the time dependence of generation for $\nu_m = 6.6$; the repetition rate is close to ν_r and equal to $\nu_m/3$.

The possibilities of increasing the amplitude of the periodic pulses $\bar{I}$ are associated with a change in the AOM operating regime, for example, the replacement of the harmonic change $\kappa_d(\tau)$ by a periodic sharp decrease in its magnitude. In this case, in order to ensure a sufficiently high inversion before the onset of each pulse, the frequency of such modulation must be reduced relative to the frequency ν_r. The generation pulse at such a change in κ_d is shown in Fig. 8a for the modulation frequency $\nu_m = 1$. One can see that the pulse amplitude

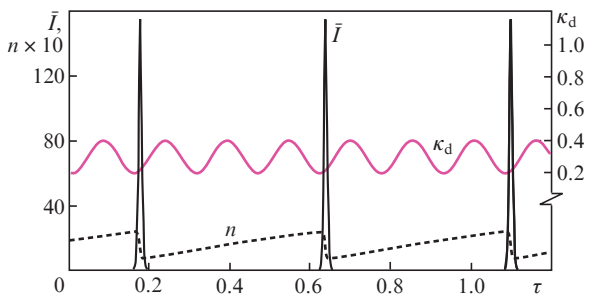

Figure 7. Generation at the modulation frequency $\nu_m = 6.6$.

is substantially higher than that under harmonic modulation when the medium is saturated deeper. The amplitude value of $\bar{I}$ is reached during the time approximately equal to $3 \times 10^{-2}\tau$; during this time interval the pulse rises from the level of spontaneous emission up to a maximum value of 600 (in the self-oscillation regime this value is ~40, see Fig. 5). The spectral composition of such a pulse determines the characteristics of mode locking. The distribution of E_j^2 in the modes cannot be established during the above-mentioned time interval. Such distributions are shown in Fig. 8b at the time moments τ (indicated by numbers 1–6 in Fig. 8a), when $\bar{I}$ is already not too small. The distribution maximum gradually shifts to the right, and the spectrum remains much narrower than that which would have occurred in the regime of stationary $\bar{I}$ (cf.

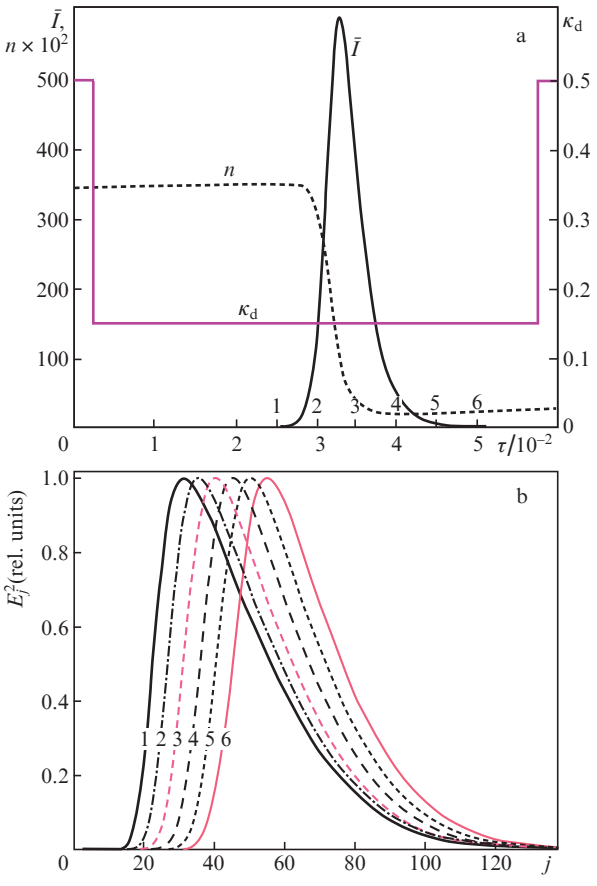

Figure 8. (a) Generation pulse with a sharp periodic decrease in the coefficient κ_d and $\nu_m = 1$ and (b) spectral profiles of the modes E_j^2. Numbers 1–6 show the time moments of the profile measurements.

with the data in Fig. 2). The results obtained indicate that the spectrum formation time corresponding to the new value of κ_d is approximately an order of magnitude greater than the pulse formation time in the Q-switching regime.

3.3. Characteristics of mode-locked pulses

In the QML regime, the amplitude distribution in a series of mode-locked pulses separated by the time interval T_c coincides in form with $\bar{I}(\tau)$. In the self-oscillation regime, their maximum amplitude, with other conditions being equal, is determined by the magnitude of the diffraction coupling coefficient. With increasing κ_d, the number of synchronising modes (according to Fig. 2) increases and at the same time the losses also increase. Therefore, just as for the value of $\bar{I}_{max}$, there exists an optimal value of κ_d, at which the highest amplitude I_{max} is attained. In this case, the effect of the increase in the number of modes is stronger, and the optimal value $\kappa_d \approx 0.17$ is somewhat larger than that for $\bar{I}_{max}$. At this value of κ_d and pumping $\eta = 5.5$, in the self-modulation regime we obtain $I_{max} = 4.5 \times 10^3$. In the case of κ_d modulation (see Fig. 8), the result is higher: $I_{max} = 5 \times 10^4$. A mode-locked pulse shown in Fig. 9 has a duration close to $\tau_p = 5 \times 10^{-7}$ in both cases (in absolute units with the chosen parameters $T_p = 10^{-10}$ s). Comparison of the pulse width with the value of T_c shows that ~100 modes are synchronised.

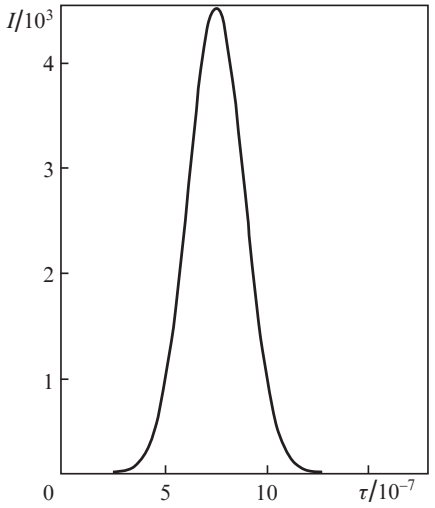

Figure 9. Mode-locked pulse.

The latter remark is connected with a possible detuning of the doubled AOM operating frequency from the intermode interval. As the detuning increases, the self-oscillation parameters change. Already for $\delta\hat{\omega} \approx 6.3$ (which in absolute units corresponds to $\delta\nu \approx 5$ kHz), an increase in the relaxation frequency, associated with a decrease in the medium saturation depth by each pulse, becomes noticeable. For this reason, the amplitude of the self-oscillation pulses $\bar{I}(\tau)$ decreases and their duration increases. The frequency composition undergoes significant changes. The value of $\Delta\Phi_j$ for each mode changes during the pulse (a smooth decrease in the difference $\Delta\varphi_j = \varphi_{j-1} - \varphi_j$ with time is only approximately compensated for by the growth of $\delta\hat{\omega}\tau$). Changes in $\Delta\Phi_j$ lead to the fact that in presence of detuning, changes in the E_j^2 distribution with time are observed – minima and maxima appear, while the effective number of operating modes decreases. At $\delta\nu \approx 10$ kHz, the regularity of the self-oscillation pulses is violated.

The scenario of the change in the structure of mode-locked pulses with increasing $\delta\nu$ has not been studied in detail. However, the changes in the E_j^2 distribution occurring during the self-oscillation pulse significantly affect the characteristics of mode-locked pulses. The amplitudes decrease, and the pulse durations increase. At the detuning $\delta\nu = 5$ kHz, the pulse is broadened to $T_p \approx 2 \times 10^{-10}$ s, and a further increase in detuning leads to a virtually proportional increase in duration. Thus, the shape of pulses acquires ruggedness close to that obtained in the simulation of modes with a random phase variation from 0 to $\pi/2$ on both sides of zero.

4. Conclusions

A model is proposed for the description of a solid-state laser with a single travelling wave AOM in a resonator. Dynamic coupling of the modes is realised by means of the field injection from the previous mode to the subsequent one with a frequency shift equal to the intermode interval. It is found that in a fairly wide range of changes in the diffraction coupling coefficient κ_d and the pump rate, the regime of generation with an averaged stationary intensity proves unstable. The instability leads to a self-oscillating QML regime with a pulse repetition rate close to the system's relaxation frequency ν_r. It is shown that the coefficient κ_d is a control parameter that can drastically change the system dynamics with the other parameters being unchanged.

Control over the characteristics of the repetitively pulsed regime by means of external periodic modulation of the coefficient κ_d at a relatively low frequency ν_m has certain features related to the impact of the relaxation resonance. Regular repetitively pulsed generation occurs in the frequency bands near ν_r when the frequency ratio ν_m/ν_r is an integer. These bands correspond to certain ranges of ν_m variation, in the intervals between which the regimes with a complicated period and chaotic generation are observed.

The coefficient κ_d not only determines the resonator loss and the injection rate, but also significantly affects the composition of mode generation, thereby to a large extent determining the shape and amplitude of the pulses of the synchronised modes.

References

1. Kuizenga D.J. *IEEE J. Quantum Eltctron.*, **17**, 1694 (1981).
2. Kornienko L.S., Kravtsov N.V., Nanii O.E., Shelaev A.N. *Sov. J. Quantum Electron.*, **11**, 1557 (1981) [*Kvantovaya Elektron.*, **8**, 2552 (1981)].
3. Kravtsov N.V., Magdich L.N., Shelaev A.N., Shnitser P.I. *Pisma Zh. Tekh. Fiz.*, **9**, 440 (1983).
4. Nadtocheev V.E., Nanii O.E. *Sov. J. Quantum Electron.*, **19**, 1435 (1989) [*Kvantovaya Elektron.*, **16**, 2231 (1989)].
5. Jabczinski J.K., Zendzian W., Rwiatkowski J. *Opt. Express*, **14** (6), 2184 (2006).
6. Donin V.I., Yakovin D.V., Gribanov A.V. *Quantum Electron.*, **42**, 107 (2012) [*Kvantovaya Elektron.*, **42**, 107 (2012)].
7. Donin V.I., Yakovin D.V., Gribanov A.V. *Opt. Lett.*, **37** (3), 338 (2012).
8. Donin V.I., Yakovin D.V., Gribanov A.V. *JETP Lett.*, **101**, 783 (2015) [*Pis'ma Zh. Eksp. Teor. Fiz.*, **101**, 881 (2015)].
9. McDuff O.P., Yarris S.E. *IEEE J. Quantum Electron.*, **3**, 101 (1967).
10. Hjelme D.R., Mickelson A.R. *IEEE J. Quantum Electron.*, **28**, 1594 (1992).
11. Lariontsev E.G. *Quantum Electron.*, **24**, 191 (1994) [*Kvantovaya Elektron.*, **21**, 209 (1994].